We are IntechOpen,
the world's leading publisher of
Open Access books
Built by scientists, for scientists

4,800
Open access books available

122,000
International authors and editors

135M
Downloads

Our authors are among the

154
Countries delivered to

TOP 1%
most cited scientists

12.2%
Contributors from top 500 universities

BOOK
CITATION
INDEX
CLARIVATE ANALYTICS
INDEXED

WEB OF SCIENCE™

Selection of our books indexed in the Book Citation Index
in Web of Science™ Core Collection (BKCI)

Interested in publishing with us?
Contact book.department@intechopen.com

Numbers displayed above are based on latest data collected.
For more information visit www.intechopen.com

Design and Fabrication of a Novel MEMS Silicon Microphone

Bahram Azizollah Ganji

Department of Electrical Engineering, Babol University of Technology,
Iran

1. Introduction

A microphone is a transducer that converts acoustic energy into electrical energy. Microphones are widely used in voice communications devices, hearing aids, surveillance and military aims, ultrasonic and acoustic distinction under water, and noise and vibration control (Ma et al. 2002). Micromachining technology has been used to design and fabricate various silicon microphones. Among them, the capacitive microphone is in the majority because of its high achievable sensitivity, miniature size, batch fabrication, integration feasibility, and long stability performance (Jing et al. 2003; Miao et al. 2002; Li et al. 2001). A capacitive microphone consists of a variable gap capacitor. To operate such microphones they must be biased with a dc voltage to form a surface charge (Pappalardo and Caronti 2002; Pappalardo et al. 2002).

Typically, a cavity is etched into a silicon substrate by slope (54.74 deg) etching profiles using KOH etching to form a thin diaphragm or perforated back plate (Kronast et al. 2001; Pedersen et al. 1997; Bergqvist and Gobet 1994; Torkkeli et al. 2000; Kabir et al. 1999). The forming of a cavity or back chamber from the backside of a wafer by KOH etching is slow and boring in that several hundred micrometers of substrate must be etched to make the chamber. Moreover, the KOH etching process is not compatible with the CMOS process. Additionally, since the back plate requires acoustic holes that must be etched from the backside in the deep back volume cavity, a nonstandard photolithographic process must be used that requires the electrochemical deposition of the photoresist and an aluminum seed layer. Most surface and bulk micromachined capacitive microphones use a fully clamped diaphragm with a perforated back plate (Ning et al. 2004; Ning et al. 1996). The fabrication process is typically long, cumbersome, expensive, and not compatible with high volume processes. Furthermore, they are not small in size (Hsu et al. 1988; Chowdhury et al. 2000).

An important performance parameter is the mechanical sensitivity of the diaphragm. The mechanical sensitivity of the diaphragm is determined by the material properties (such as Young's modulus and the Poison ratio), thickness, and the intrinsic stress in the diaphragm. Very thin diaphragms are very fragile. In microfabrication, it is difficult to control the intrinsic stress levels in materials. In a prior paper (Rombach et al 2002), the stress problem was addressed by using a sandwich structure for diaphragms, in which layers with compressive and tensile stress were combined. If the diaphragm is composed of more than one material, this may induce a stress gradient because of the mismatch of the thermal expansions in the different materials. Any intrinsic stress gradient in the diaphragm

material will cause diaphragm to bend, leading to a change of the air gap in the device, and therefore the sensitivity and cut-off frequency.

The objective in this research is to overcome the disadvantages of the prior works by designing a novel MEMS capacitive microphone that utilizes a perforated diaphragm; thus achieving small size and improved microphone sensitivity by decreasing the mechanical stiffness of the diaphragm.

2. Microphone design

Capacitive microphones generally consist of a diaphragm that is caused to vibrate by impinging waves of acoustic pressure, a back plate and air gap. In its simplest form, a diaphragm is stretched over a conductive back plate and supported by post so that there is a gap between the membrane and the back plate. Figure 1 shows the basic structure of the condenser microphone. A diaphragm is stretched by a tensile force, T, is put in front of a fixed conducting back plate by means of a surrounding border which assures a separation distance, d, to create a capacitance with respect to the back plate and biased with a DC voltage. An acoustic wave striking the diaphragm causes its flexural vibration and changes the average distance from the back plate. The change of distance will produce a change in capacitance and charge, giving rise to a time varying voltage, V, on the electrodes.

This structure works as a condenser whose static capacitance is (Pappalardo et al. 2002):

$$C = \varepsilon_0 \frac{A}{d} \tag{1}$$

where ε_0 is the dielectric constant of the air and A is the surface area of the metallized membrane.
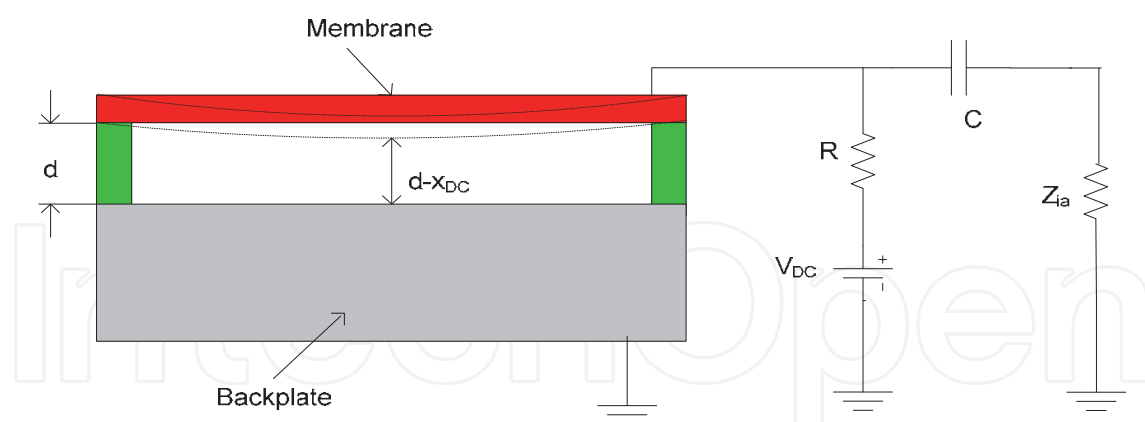

Fig. 1. Basic structure of the condenser microphone

When a DC voltage V_{DC} is applied between the two electrodes, an electric charge $Q_{DV} = C_0 V_{DC}$ appears on the surface of the membrane, where

$$C_0 = \frac{\varepsilon_0 A}{(d - x_{DC})} \tag{2}$$

accounting for the gap height variation due to the bias voltage, and x_{DC} is the static average displacement due to the DC electrostatic force. In reception, an acoustic wave striking the

membrane causes its flexural vibration and changes the average distance from the back plate, which becomes

$$x = d - x_{DC} + x_{ac} = d_0 + x_{ac} \tag{3}$$

where x_{ac} is the dynamic average displacement of the vibrating membrane. As a consequence, the change of distance will produce a change in capacitance and charge, giving rise to a time varying voltage V on the electrodes.

$$V = \frac{Q}{C} = \frac{Q.x}{\varepsilon_0.A} \tag{4}$$

In the small signal approximation, using first order Taylor expansion around the bias point (V_{DC}; d_0) we have,

$$V_{ac} = \left|\frac{\partial V}{\partial Q}\right|_{bias} Q_{ac} + \left|\frac{\partial V}{\partial x}\right|_{bias} x_{ac} = \frac{d_0}{\varepsilon_0 A} Q_{ac} + \frac{Q_{DC}}{\varepsilon_0 A} x_{ac} \tag{5}$$

Where V_{ac} and Q_{ac} are voltage and charge signal components and Q_{DC} the polarization charge. For this reason the surface electrical charges are forced to move giving rise to a small alternating current which flows in the pre-amplifier input resistance Z_{ia}, through the condenser C.

In this research, 2 types of MEMS capacitive microphone have designed and fabricated on 4 inches silicon wafer. First design is microphone with clamped perforated diaphragm (see Fig. 2). The novelty of this method relies on diaphragm includes some acoustic holes to reduce air damping in the gap. Compared with previous works, the chip size of this microphone is reduced; the complex and expensive fabrication process can be avoided by making acoustic holes in diaphragm. Second design is microphone with slotted perforated diaphragm (see Fig. 3). The novelties of this method relies on the diaphragm includes some slots to reduce the effect of residual stress and stiffness of diaphragm and also includes some acoustic holes to reduce air damping in the gap. By this way, the microphone size was reduced, and the sensitivity was increased.

In next section, the behaviors of the microphones with clamped and slotted perforated diaphragms are analyzed using the finite element method (FEM).
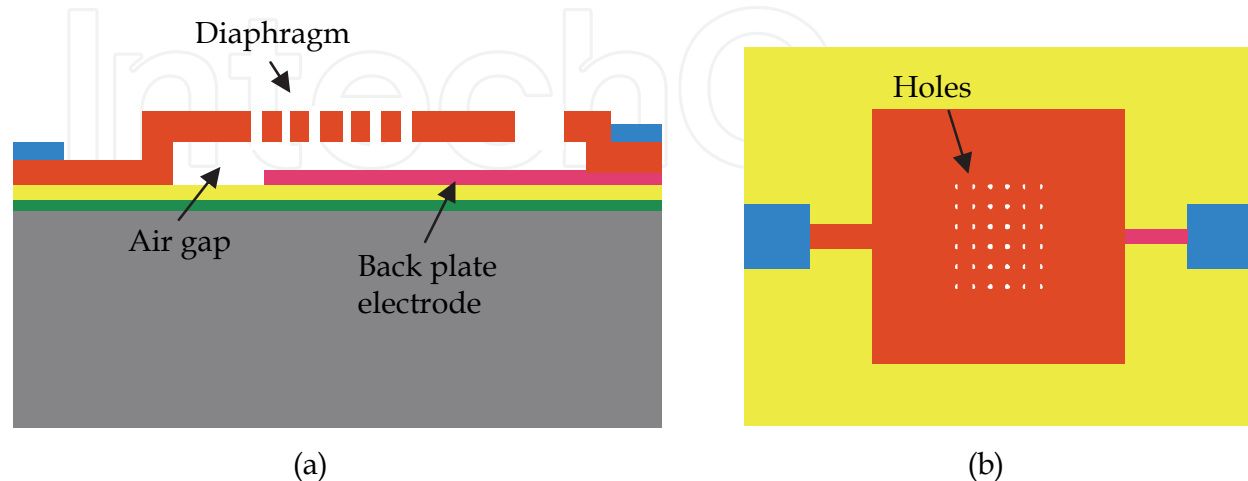

Fig. 2. (a) Cross-section, and (b) top view of clamped perforated microphone (Ganji and Majlis 2009)
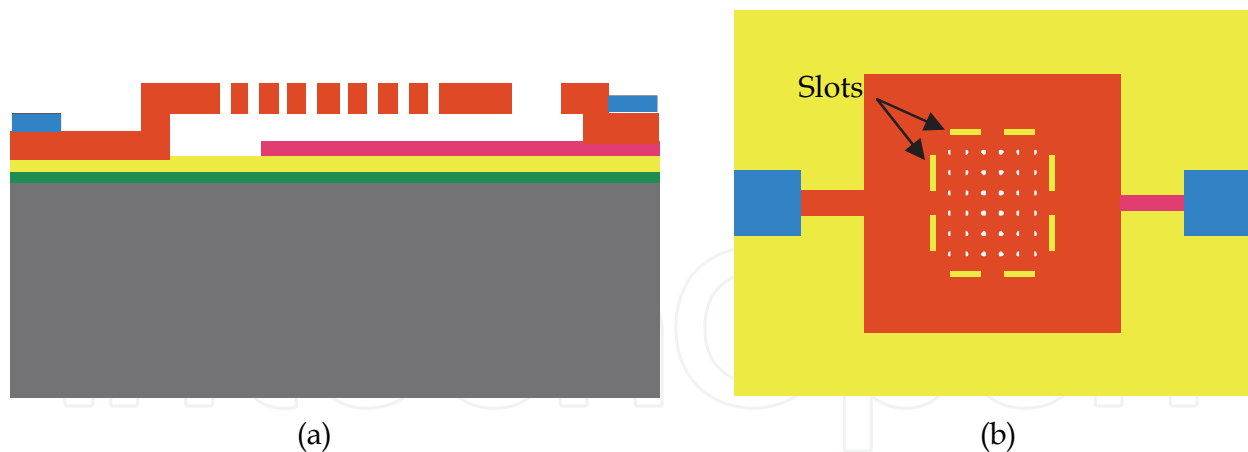
(a)   (b)

Fig. 3. (a) Cross-section, and (b) top view of slotted perforated microphone (Ganji and Majlis 2009)

3. Finite element analysis (FEA) of the microphone

The analysis objectives are:
1. To verify the deformation of the diaphragm due to the electrostatic attraction force between the diaphragm and backplate, and the mechanically applied force
2. To verify the capacitance between the diaphragm and the back plate

The analysis options are nonlinear analysis, accuracy of convergence that is 0.001 μm, and a maximum mesh size that is 2.4% of *X-Y* dimension. Figure 4a shows the simulation setup of the microphone with clamped diaphragm. Silicon wafer faces and 4 lateral faces of the poly silicon diaphragm are fixed. Figure 4b shows the simulation setup for the microphone with slotted diaphragm. Silicon wafer faces and 8 lateral faces of arms are fixed. A DC bias voltage is provided between the diaphragm and the back plate.

Figure 5 show the stress distribution over of the clamped diaphragm (Fig. 5a) and the slotted diaphragm (Fig. 5b) using the FEM. We can see that the stress concentration is found at the edges of the clamped diaphragm. For the slotted diaphragm, however, the value of stress at the center and edges of the diaphragm is very low and it increases as it goes to the suspending area.

Figure 6 shows deformation in the *Z* axis of the diaphragm with a thickness of 3 μm and an initial stress of 20 Mpa at an applied pressure of 1.5 kPa. Figure 6a shows the maximum central deflection of clamped diaphragm is 0.245 μm and Figure 6b shows the maximum deflection of slotted diaphragm is 0.6643 μm. We can see that the slotted diaphragm has more deflection than the clamped one under same load.

Figure 7 shows the simulated diaphragm deflection versus voltage and Figure 8 show the simulated diaphragm deflection versus pressure for the clamped diaphragm (2.43 x 2.43 mm²) and the slotted diaphragm (1.5 x 1.5 mm²). According to the results, both microphones have the same pull-in voltage (7 V) and the same high mechanical sensitivity (53.3 nm/Pa), however the slotted microphone is at least 1.62 times smaller than the clamped structure.

Figure 9 shows the central deflection versus bias voltage of the clamped and slotted microphones using a 0.5-mm square diaphragm with a thickness of 3 μm, an air gap of 1 μm, and a diaphragm stress of 1500 MPa (Ganji and Majlis 2009). We can see that the pull-in voltage for the clamped diaphragm is 105 V, and that for the slotted diaphragm is 49 V. We can see that, by introducing slots in microphone, the diaphragm stiffness decreased, therefore the pull-in voltage decreased about 53%.
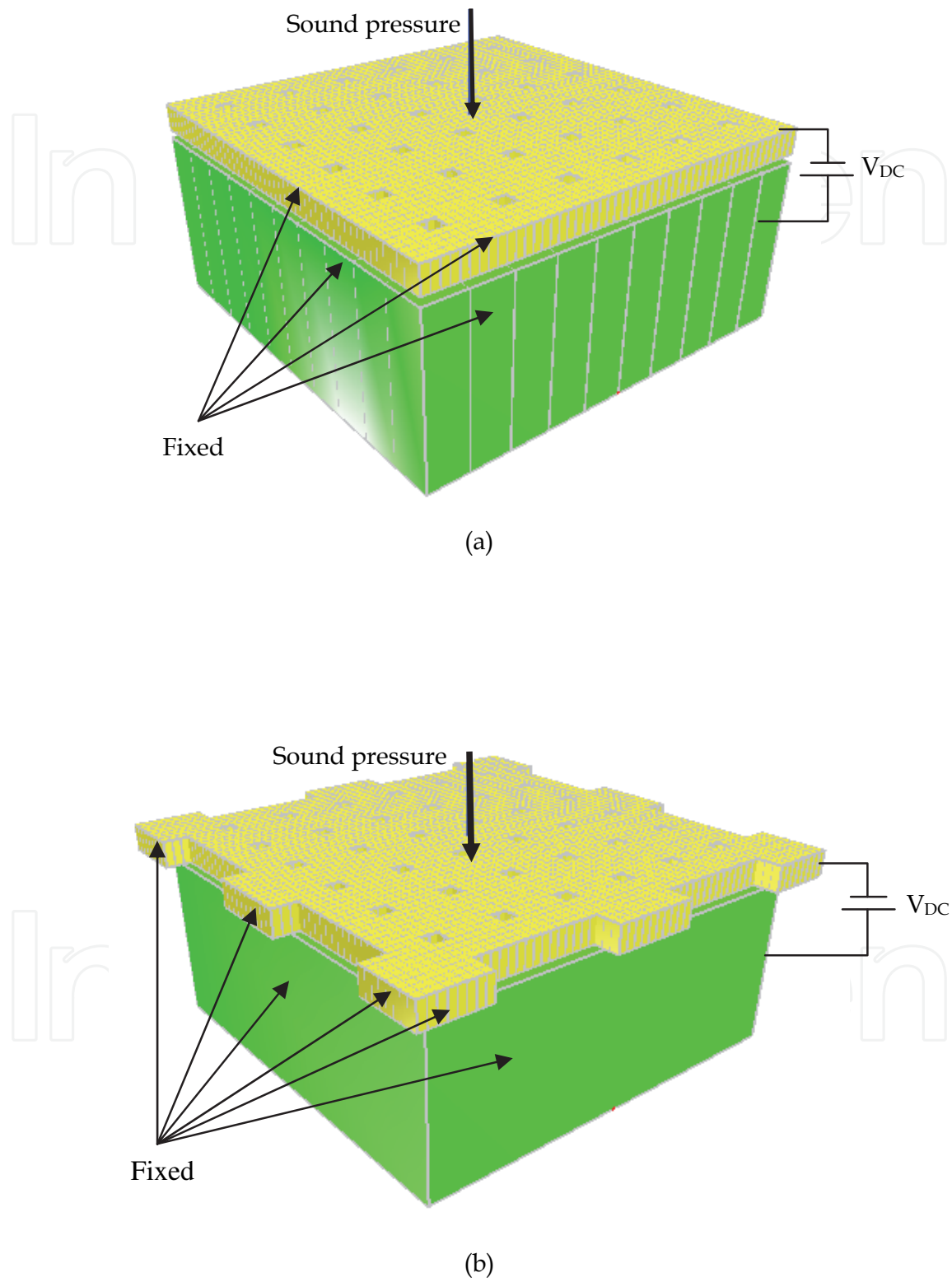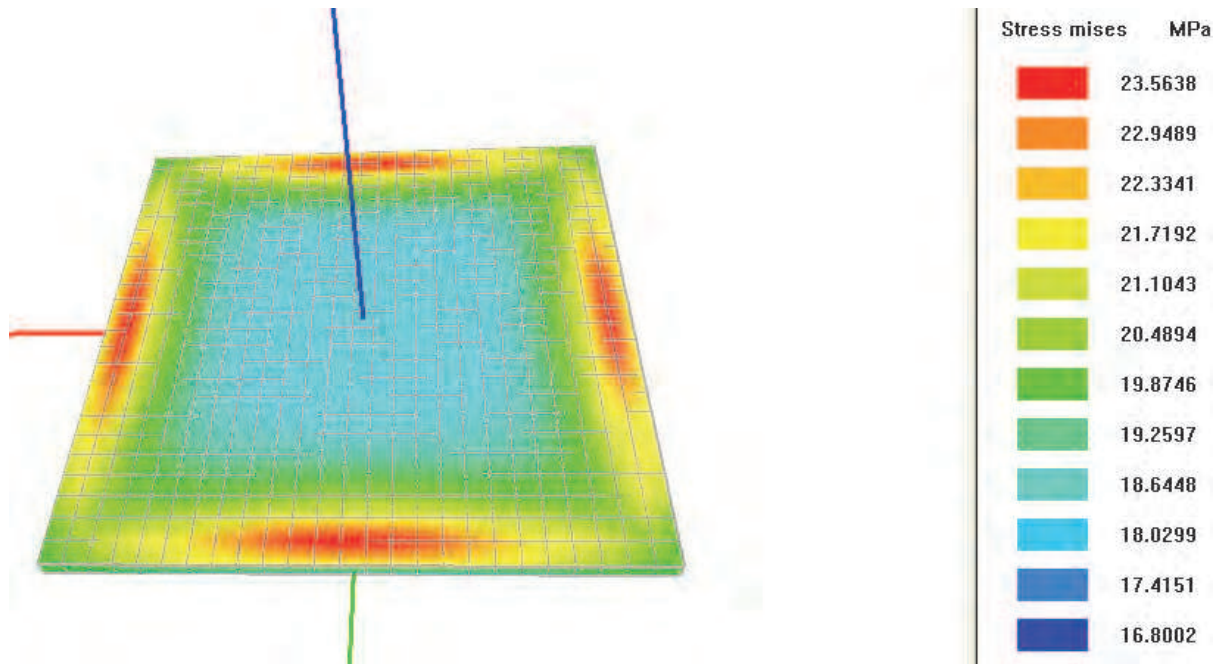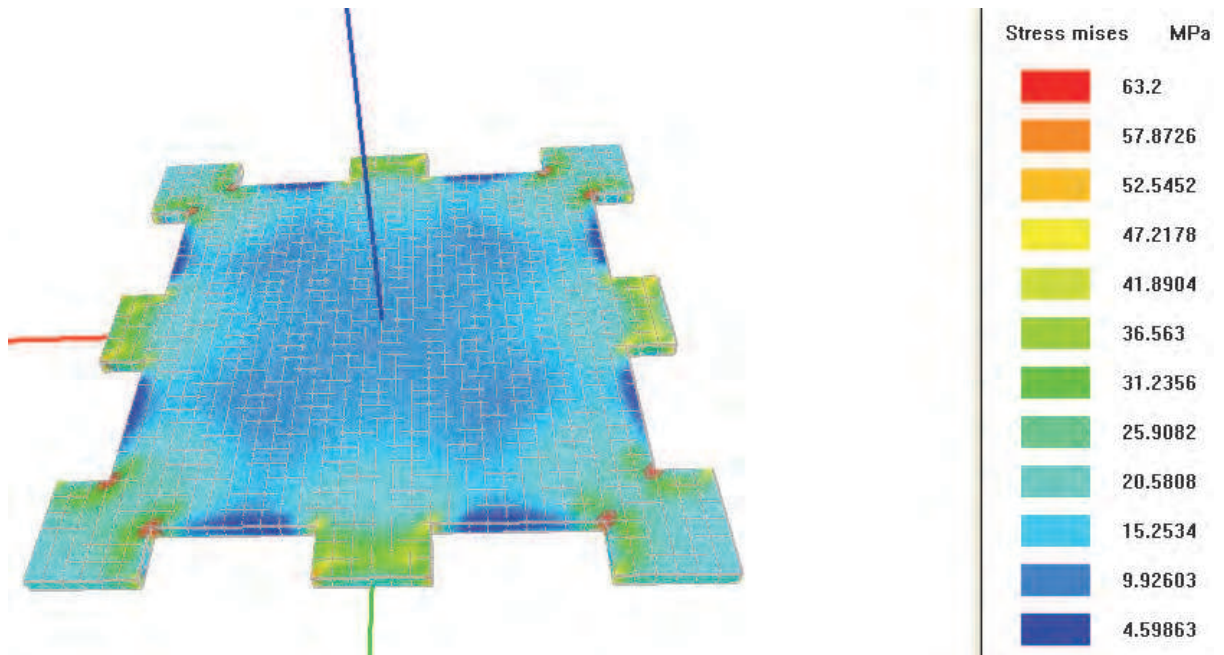
(a)

(b)

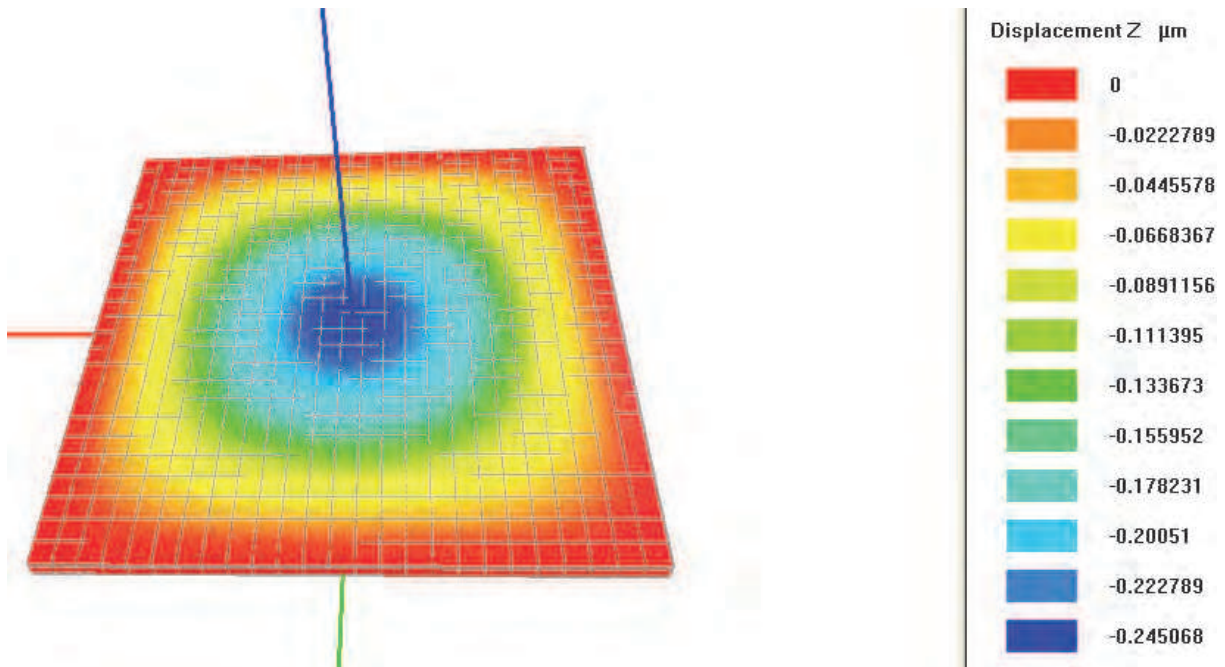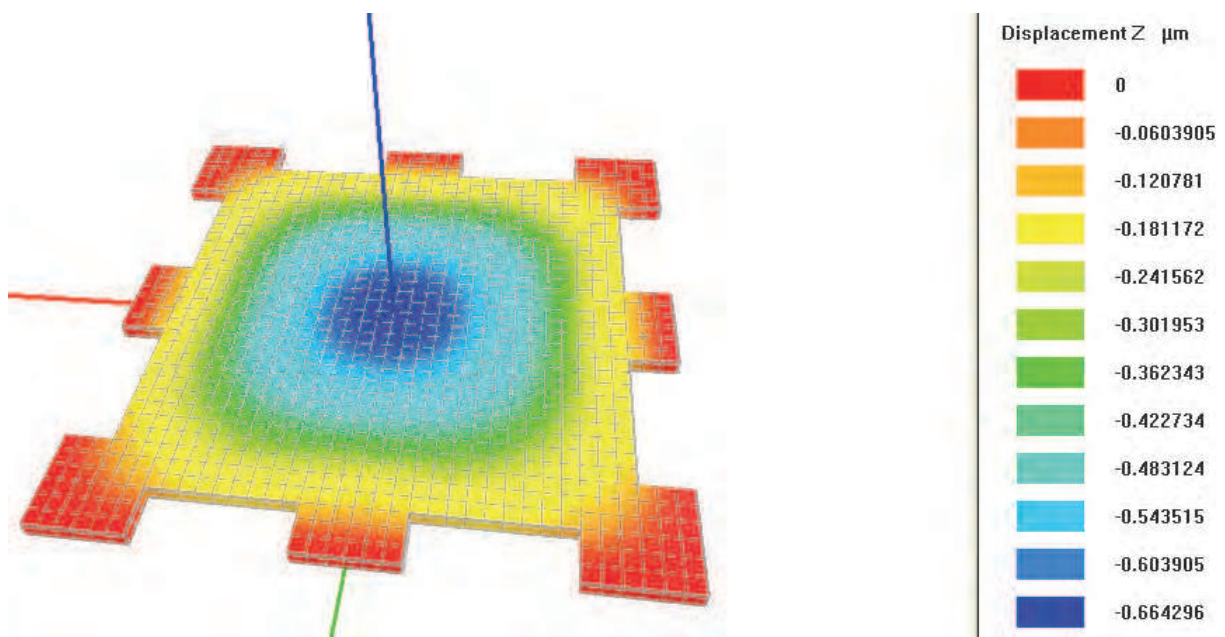Fig. 4. Simulation setup for (a) clamped microphone, (b) slotted microphone

(a)

(b)

Fig. 5. Stress distribution on the (a) clamped diaphragm and (b) slotted diaphragm

(a)

(b)

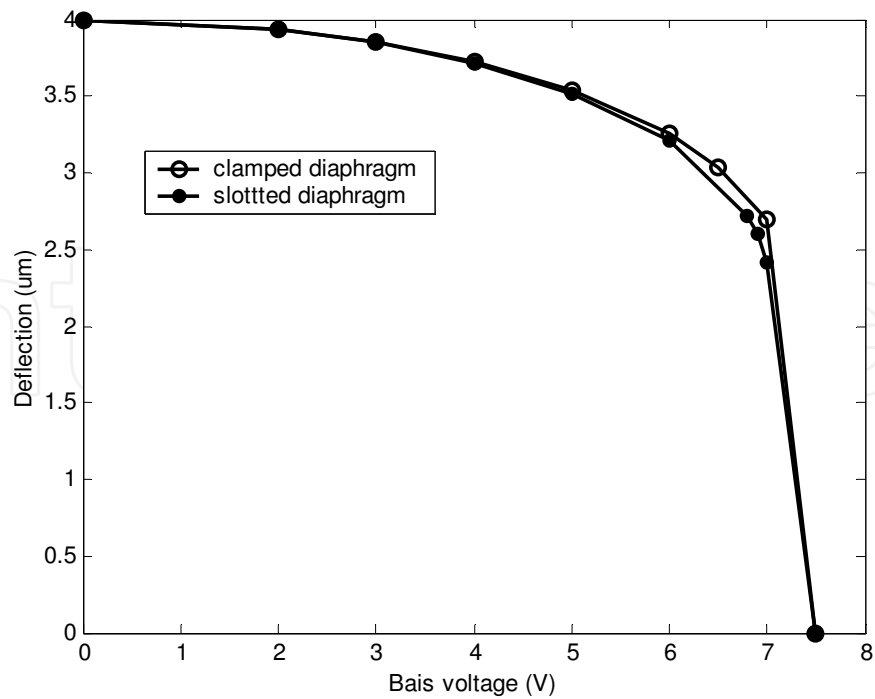Fig. 6. Diaphragm deformation on the Z axis of the (a) clamped diaphragm and (b) slotted diaphragm
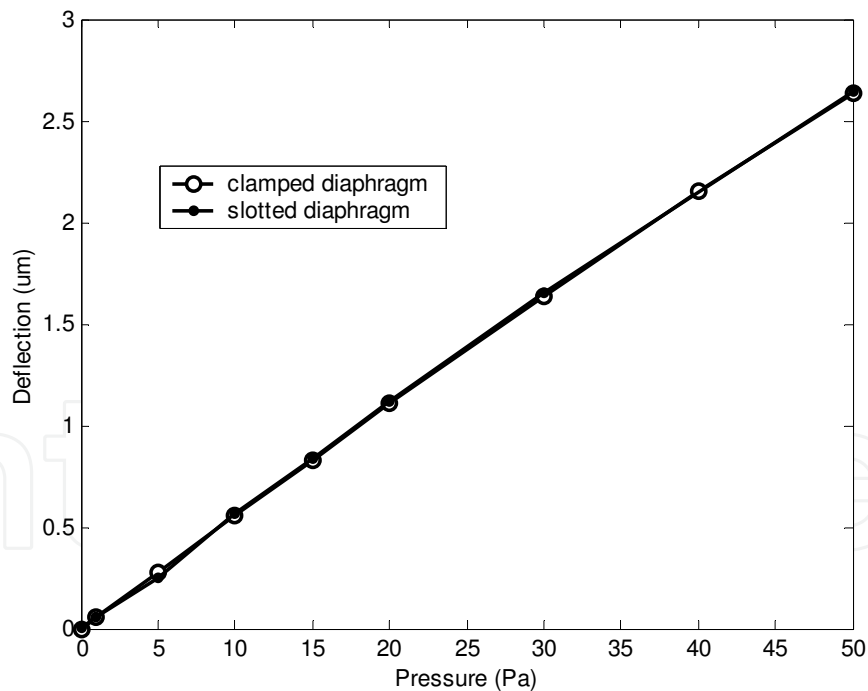
Fig. 7. Diaphragm deflection versus voltage

Fig. 8. Diaphragm deflection versus pressure

Figure 10 shows the relation between capacitance and pressure for clamped and slotted microphones under 60% of pull-in voltage. The results yield a sensitivity ($S=\mathrm{d}C/\mathrm{d}P$) of 5.33×10^{-6} pF/Pa for the clamped and 3.87×10^{-5} pF/Pa for the slotted microphones. By introducing the slots in the diaphragm, the sensitivity's increased 7.27 times. The first resonance frequency of the diaphragm is 1.11 MHz for the clamped and 528.57 kHz for the

slotted microphones. From the preceding analysis, we can conclude that there is a dilemma between the high sensitivity and high resonance frequency. For all the diaphragms, to satisfy most of the microphones, the first resonance frequency of the diaphragm should be well above 20 kHz (hearing range).
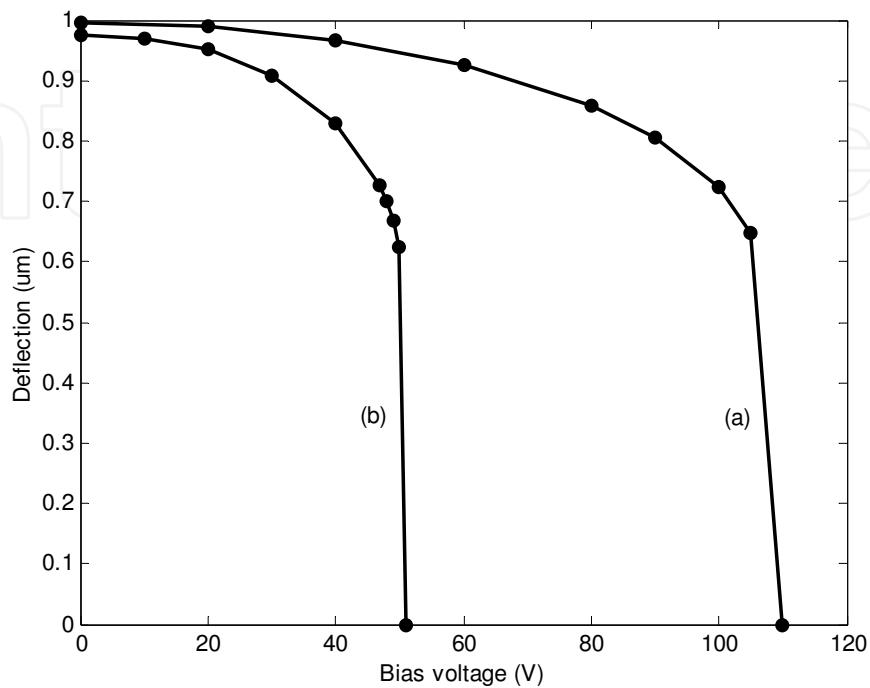

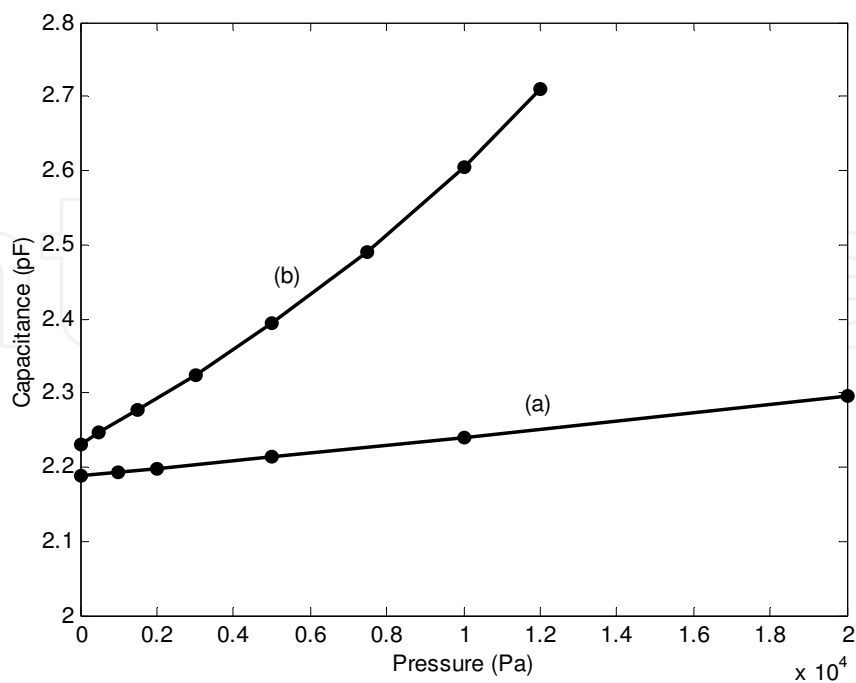Fig. 9. Central deflection of a (curve a) clamped and (curve b) slotted diaphragm versus bias voltage

Fig. 10. Capacitance versus pressure for (a) the clamped and (b) the slotted microphones

4. Fabrication of microphone

This section will describe how the microphone was fabricated on silicon wafer. In this process, sputtered aluminum is used as a diaphragm and back plate electrode, resist (AZ1500) as a sacrificial layer, and sputtered silicon oxide as an insulation layer. The whole process sequence uses three masks and several deposition, and etching processes. The process starts with a single side polished silicon wafer as a substrate. The major fabrication steps are shown in Figure 11, and described as follows:

First a 4-inch silicon wafer should be cleaned using standard cleaning procedure to remove organic contaminants such as dust particles, grease or silica gel and then remove any oxide layer from the wafer surface prior to processing. The first step in the cleaning process is to clean the wafer using ultrasonic in the acetone solution for 5 minutes. The second step is to put the wafer into the methanol solution using ultrasonic for 5 minutes. Final step is to dip the sample in a 10:1 DI water-HF solution (10% HF) until hydrophobic (i.e. no water can stick to wafer). This will remove native oxide film (see Fig. 11a).

Then a 2 μm thick silicon oxide is sputtered on clean silicon wafer as an insulation layer (see Fig. 11b). Next, a 0.5 μm Al has been sputtered on silicon oxide as a back plate electrode. It was then patterned using photoresist mask and etched by Al etchant for 5 minutes (see Fig. 11c). The etch rate of sputtered Al in Al etchant is 60 nm/minute. Etchant for aluminum is 16:4:1 of phosphoric acid (H_3PO_4), DI water, and nitric acid (HNO_3). After that, a 1.3 μm thick resist (AZ1500) was deposited and patterned in order to form a sacrificial layer (see Fig. 11d). Resist can be easily deposited and removed using acetone. Moreover, acetone has a high selectivity to resist compared to silicon oxide and Al, thus it completely removes sacrificial resist without incurring significant damage silicon oxide and Al. Sacrificial resist is usually deposited by spin coater. Baking is the most important. The main purpose of baking is to remove solvent from resist. A few minutes of hot plate baking temperature of at least $100°C$ is required to evaporate the solvent. The samples are then heated at$145°C$ for 3 minutes.

Then, a 3 μm thick layer of aluminum is sputtered on resist sacrificial layer as a material of diaphragm (see Fig. 11e). The Al layer is then patterned using positive resist mask to define the geometry of the diaphragm, contact pad, and anchors. After that the structure was immersed in Al etchant for 35 minutes to etch the Al for making diaphragm structure. The approximate etch rate of Al in acetone in room temperature is zero. Therefore acetone shows a high selectivity against Al.

Finally, the sacrificial resist layer is etched using acetone to release the diaphragm (see Fig. 11f). The fabrication process is completed by immersing it in deionized water (DI) and then acetone. Next, the whole structure is dried on hot plate at $60°C$ for 90 seconds to protect the diaphragm from sticking to the back plate.

After all processing on the wafers were completed, the last step was to determine if the fabrication process had been successful. It is important to observe the silicon membrane and check to ensure that the resist layer was removed. All testing was performed by using a Scanning Electron Microscope (SEM) and optical microscope to capture images of the membrane surface and images of the cross-section. Figure 12 shows the optical microscopy top view of Al back plate electrode and photoresist (AZ1500) sacrificial layer on silicon oxide.

Figure 13(a) shows the surface of the fabricated clamped microphone and Figure 13(b) shows the close up view of the Al diaphragm surface (0.5x0.5 mm²) with acoustic holes using SEM. Figure 14 shows the SEM image of slotted microphone with 8 slots and 8 arms. Figure 15 show the sacrificial layer etching with diaphragm thickness of 3µm, and air gap of 1.3µm. It can be seen that, sacrificial layer has been removed under Al membrane completely, and Al membrane has been released.

The measured pull-in voltage for clamped microphone is 51 V, however the measured pull-in voltage of slotted microphone with sputtered aluminum diaphragm is 25 V. It can be seen that, by introducing slots in microphone, the diaphragm stiffness decreased, therefore the pull-in voltage about 50% decreased. Consequently, it causes the microphone sensitivity is increased.
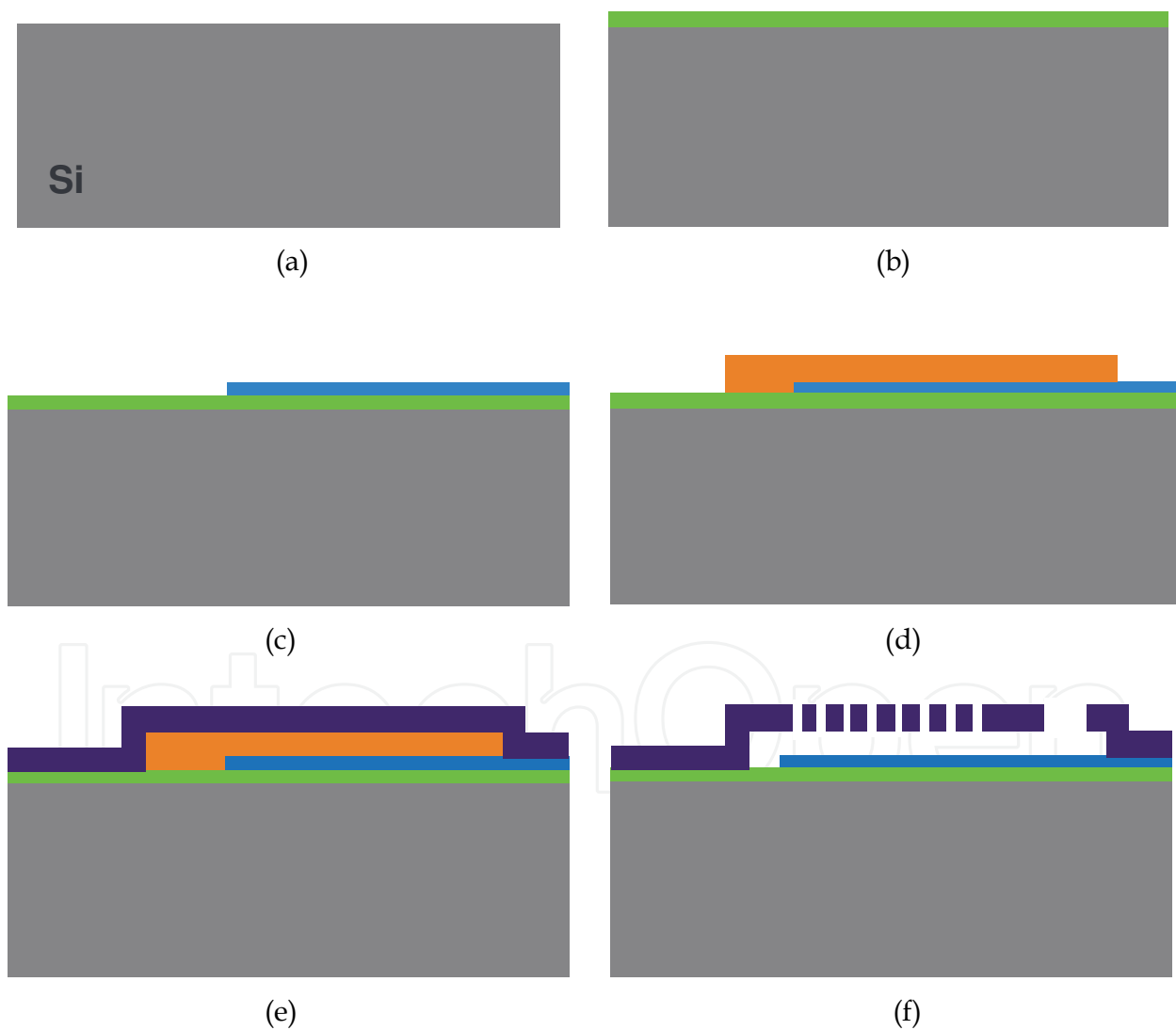

Fig. 11. Process flow of the microphone (Ganji and Majlis 2010)
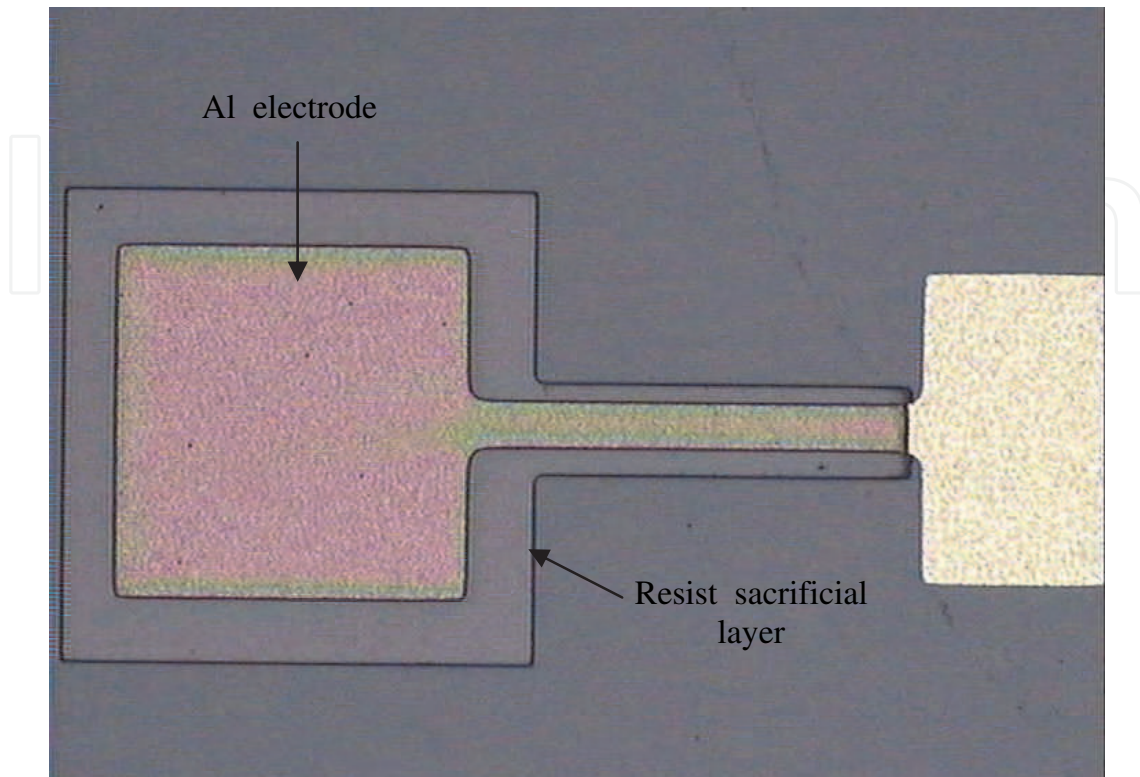
Fig. 12. Top view of Al back plate electrode and photoresist sacrificial layer on silicon oxide
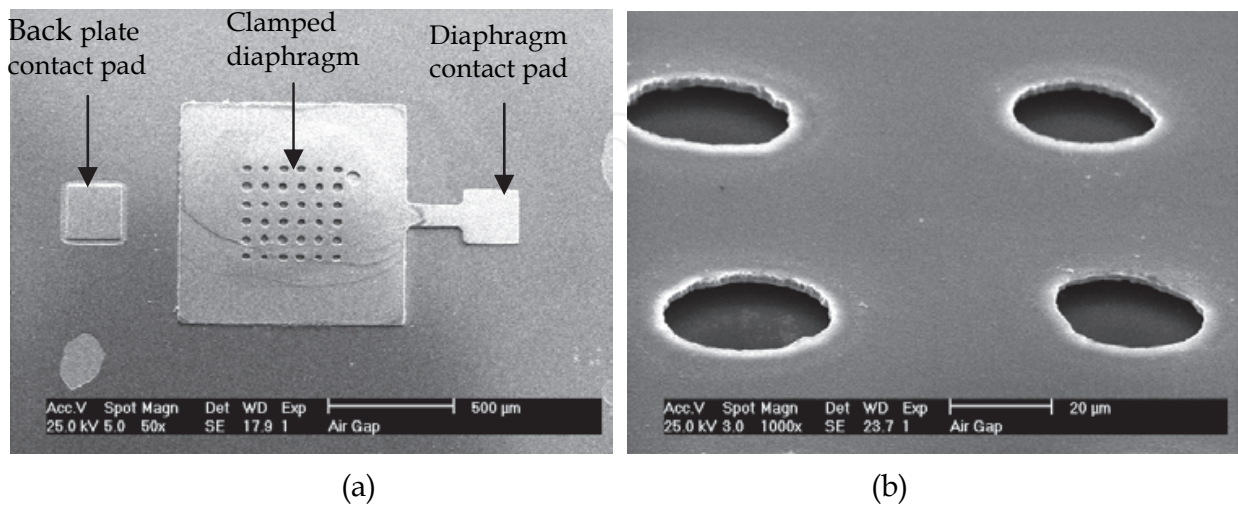

Fig. 13. (a) Surface of the clamped microphone, (b) close up view of the diaphragm

(a)   (b)
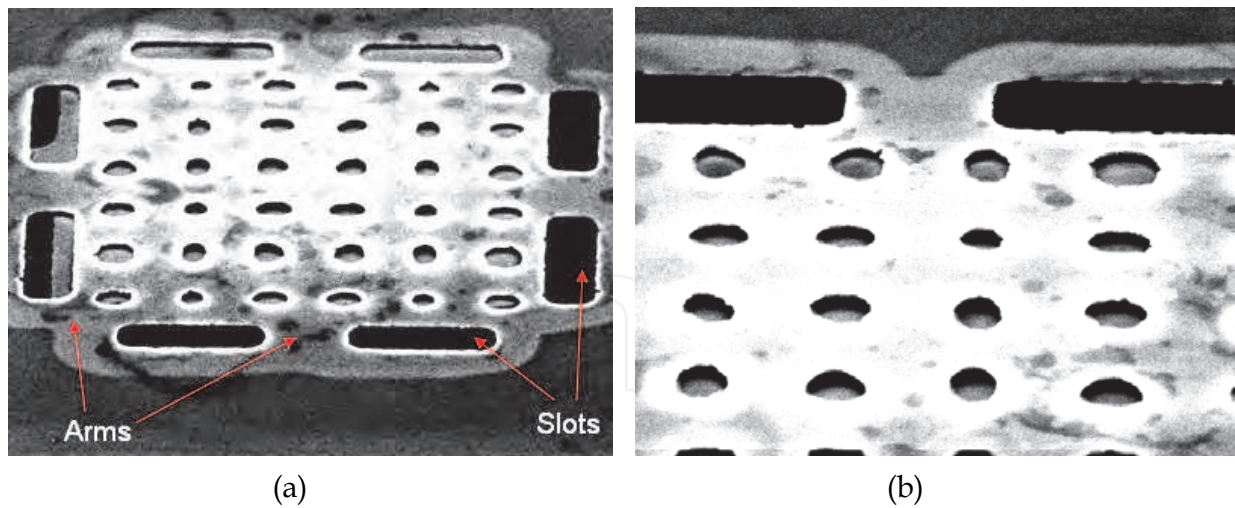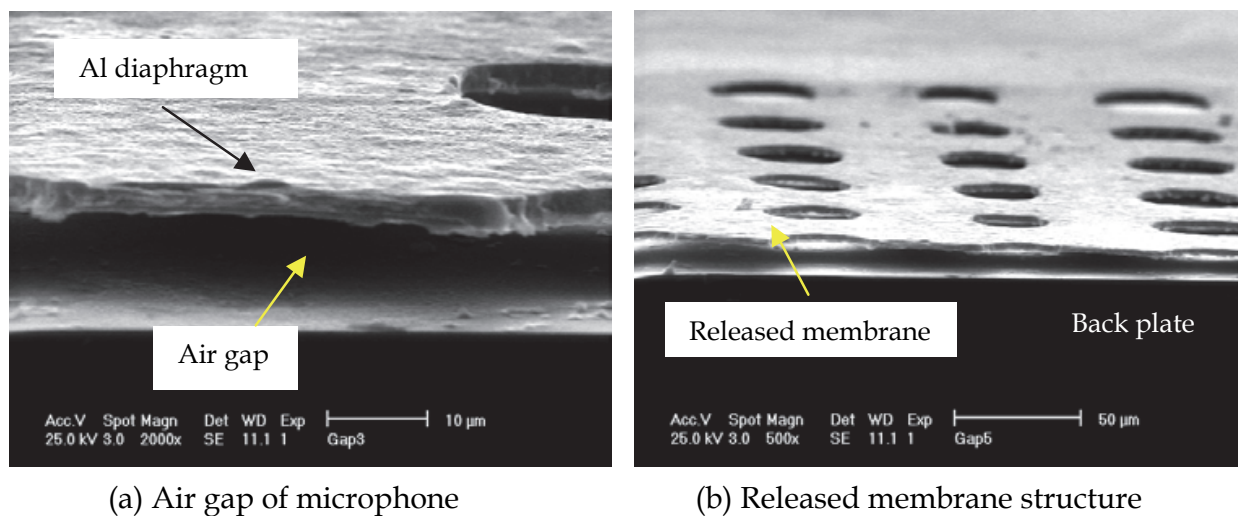
Fig. 14. SEM picture of (a) slotted microphone, (b) close up view of diaphragm

(a) Air gap of microphone   (b) Released membrane structure

Fig. 15. Cross-section view of the microphone structure using SEM machine (Ganji and Majlis 2009)

5. Test of microphone

Figure 16 shows the MEMS capacitive microphone has been connected to amplifier, power amplifier and speaker. The bias voltage of microphone, V_b, is 3 V, and bias resistance, R_b, is 100MΩ. The amplifier consists of an operational amplifier LF347 with high input impedance of 10^{12} Ω, R_f of 1 MΩ, R_s of 1.25 KΩ, and Vcc of 9 V battery. The voltage gain of amplifier, ($A_{v1} = R_f/R_s$) is 800. The power amplifier is a mini amplifier-speaker CAT. No. 277-1008C. The voltage gain of power amplifier, A_{v2}, is 50. The total voltage gain of external amplifier, ($A_{vtot} = A_{v1}.A_{v2}$) is 40000. Figure 17 shows the 2 seconds of a speech signals are applied to the microphone. It can be seen that the external amplifier was able to detect the sound waves from microphone on oscilloscope. From the figure, the maximum amplitude of output speech signal of amplifier is 45 mV, thus the maximum output of microphone is 1.125 µV.
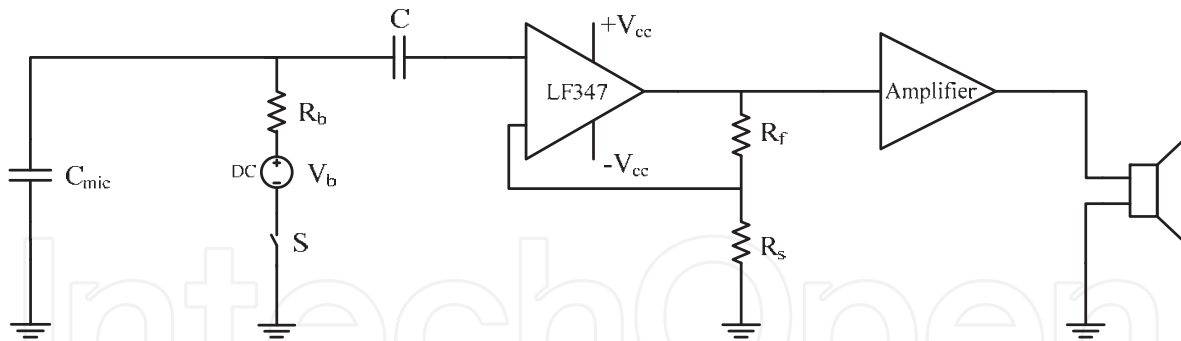
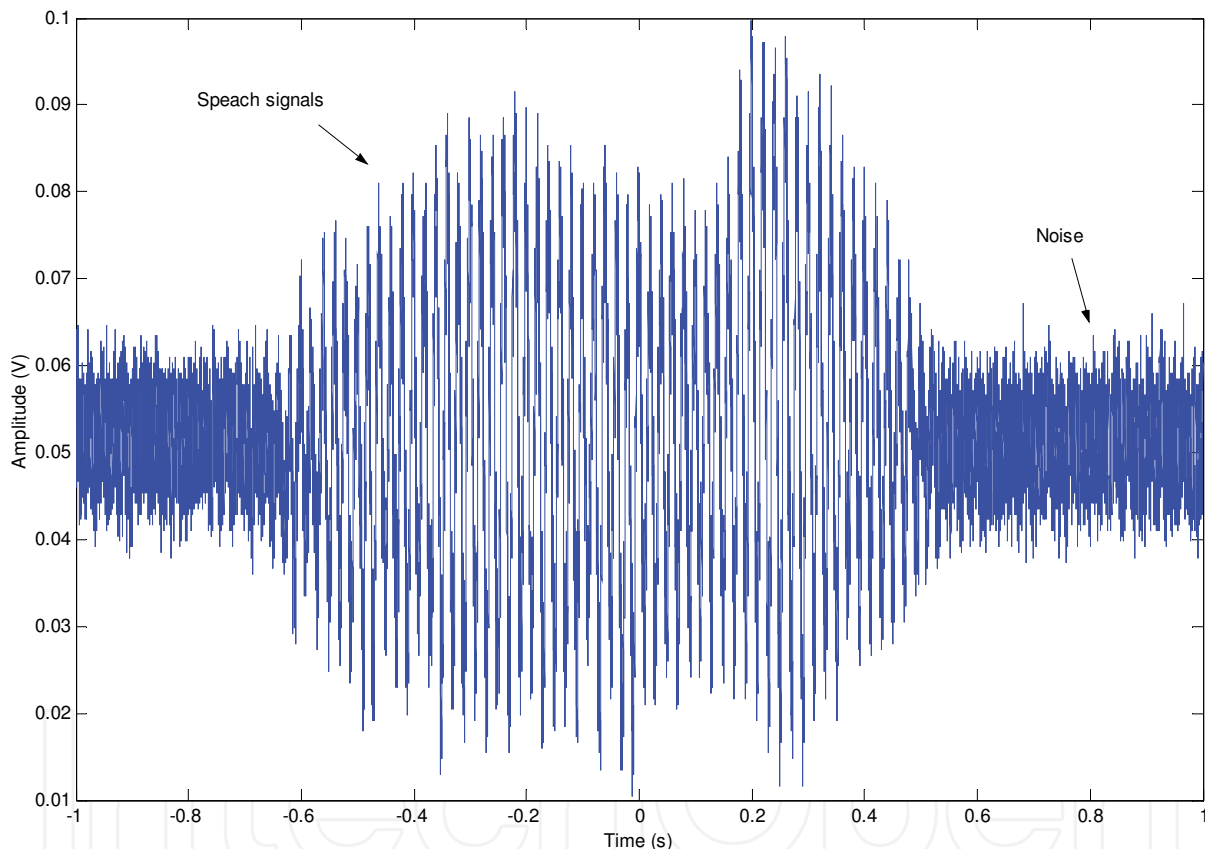Fig. 16. Circuit diagram of external amplifier which connected to microphone (Ganji and Majlis 2010)

Fig. 17. 2 seconds of speech signals are applied to the microphone

6. Conclusion

A novel MEMS capacitive microphone was designed, and fabricated with a small size and a high sensitivity. The device used a perforated diaphragm, mono crystalline silicon back plate, and resist as a sacrificial layer. The results show the obvious improvement in size and sensitivity of the slotted microphone compared with the clamped one. According to the results, the slotted microphone with a 1.5-mm diaphragm width, at least 1.62 times is smaller than the clamped structure with a 2.43-mm diaphragm width. The results also yield a sensitivity of 5.33 $\times 10^{-6}$ pF/Pa for the clamped and 3.87 $\times 10^{-5}$ pF/Pa for the slotted

microphones using a 0.5-mm square aluminum diaphragm with a thickness of 3 μm and an air gap of 1 μm. We can see that, by introducing the slots in the diaphragm, the microphone sensitivity was increased 7.27 times. The measured pull-in voltage for the clamped microphone with sputtered aluminum diaphragm is 51 V, however, the pull-in voltage of the slotted microphone is 25 V. This means that the slotted diaphragm stiffness has been decreased; consequently, the pull-in voltage decreased about 50%. The microphone has been tested with external amplifier and speaker, it can be seen that the external amplifier was able to detect the sound waves from microphone on speaker. The maximum amplitude of output speech signal of amplifier is 45 mV, and the maximum output of microphone is 1.125 μV.

7. References

Bergqvist, J., Gobet, J. (1994). Capacitive microphone with a surface micromachined backplate using electroplating technology. *J. Microelectromech. Syst.* 3(2): 69–75.

Chowdhury, S., Jullien, G. A., Ahmadi, M. A., Miller, W. C. (2000). MEMS acousto-magnetic components for use in a hearing instrument. *Presented at SPIE's Symposium on Design, Test Integration, and Packaging of MEMS/MOEMS, Paris.*

Ganji, B. A. and Majlis, B. Y. (2009). Design and fabrication of a new MEMS capacitive microphone using a perforated aluminum diaphragm. *Sensors and Actuators A*: Physical, 149: 29–37.

Ganji, B. A. and Majlis, B. Y. (2009). Design and fabrication of a novel single-chip MEMS capacitive microphone using slotted diaphragm. *J. Micro/Nanolith. MEMS MOEMS* 8(2), DOI: 10.1117/1.3091941, pp.021112 (1-7).

Ganji, B. A. and Majlis, B. Y. (2009). Fabrication and Characterization of a New MEMS Capacitive Microphone using Perforated Diaphragm. *International journal of Engineering,* Vol. 22, No. 2, pp. 153-160.

Ganji, B. A. and Majlis, B. Y. (2009). High Sensitivity and Small Size MEMS Capacitive Microphone using a Novel Slotted Diaphragm, *Microsystem Technology*, Vol. 15, Issue 9, pp: 1401-1406.

Ganji, B. A. and Majlis, B. Y. (2010). Slotted capacitive microphone with sputtered aluminum diaphragm and photoresist sacrificial layer, *Microsystem Technology*, Vol. 16, pp: 1803–1809.

Hsu, P. C., Mastrangelo, C. H., Wise, K. D. (1988). A high density polysilicon diaphragmcondenser microphone. *In Conf. Record IEEE 11th Int. Workshop on MicroElectro Mechanical Systems (MEMS)*, pp. 580–585.

Jing, C., Liu, L., Li, Z., Tan, Z., Xu, Y., Ma, J. (2003). On the single-chip condenser miniature microphone using DRIE and back side etching techniques. *Sens. Actuators,* A 103: 42–47.

Kabir, A. E. , Bashir, R., Bernstein, J., De Santis, J., Mathews, R., O'Boyle, J. O., Bracken, C. (1999) Very High Sensitivity Acoustic Transducers with Thin P+ Membrane and Gold Back Plate Sensors and Actuators-A, 78: 138-142.

Kronast, W., Muller, B., Siedel, W., Stoffel, A., (2001). Single-chip condenser microphone using porous silicon as sacrificial layer for the air gap. *Sens. Actuators,* A 87: 188–193.

Li, X., Lin, R., Kek, H., Miao, J., Zou, Q. (2001). Sensitivity- improved silicon condenser microphone with a novel single deeply corrugated diaphragm. *Sensors and Actuators A* 92: 257-262.

Ma, T., Man, T.Y., Chan, Y. C., Zohar, Y., Wong, M. (2002). Design and fabrication of an integrated programmable floating-gate microphone. *Proceedings of the Fifteenth IEEE International Conference on Micro Electro Mechanical Systems*, pp. 288–291.

Miao, J., Lin, R., Chen, L., Zou, Q., Lim, S. Y., Seah, S. H. (2002). Design considerations in micromachined silicon microphones. *Microelectronics Journal* 33: 21-28.

Ning, J., Liu, Z., Liu, H., Ge, Y. (2004). A silicon capacitive microphone based on oxidized porous silicon sacrificial technology. *Proc. 7th Int. Conf. on Solid-State and Integrated Circuits Technology, IEEE*, 3: 1872–1875.

Ning, Y. B., Mitchell, A. W., Tait, R. N. (1996). Fabrication of a silicon micromachined capacitive microphone using a dry-etch process. *Sens. Actuators, A* 53: 237–242.

Pappalardo, M, Caliano, G, Foglietti, V, Caronti, A, Cianci, E (2002) A new approach to ultrasound generation: the capacitive micromachined transducers. *University Roma, Rome, Italy.*

Pappalardo, M., A. Caronti (2002). A new alternative to piezoelectric transducer for NDE and medical applications: the capacitive ultrasonic micromachined transducer (cMUT). *University Roma, Rome, Italy.*

Pedersen, M., Olthuis, W., Bergveld, P. (1997). A silicon condenser microphone with polyimide diaphragm and back plate. *Sens. Actuators, A* 63: 97–104.

Rombach, P., Mullenborn, M., Klein, U., Rasmussen, K. (2002). The first low voltage, low noise differential silicon microphone, technology development and measurement results. *Sens. Actuators, A* 95: 196– 201.

Torkkeli, A., Rusanen, O., Saarilahti, J., Seppa, H., Sipola, H., Hietanen, J. (2000). Capacitive microphone with low- stress polysilicon membrane and high-stress polysilicon backplate. *Sens. Actuators* 85: 116–123.

Crystalline Silicon - Properties and Uses

Edited by Prof. Sukumar Basu

The exciting world of crystalline silicon is the source of the spectacular advancement of discrete electronic devices and solar cells. The exploitation of ever changing properties of crystalline silicon with dimensional transformation may indicate more innovative silicon based technologies in near future. For example, the discovery of nanocrystalline silicon has largely overcome the obstacles of using silicon as optoelectronic material. The further research and development is necessary to find out the treasures hidden within this material. The book presents different forms of silicon material, their preparation and properties. The modern techniques to study the surface and interface defect states, dislocations, and so on, in different crystalline forms have been highlighted in this book. This book presents basic and applied aspects of different crystalline forms of silicon in wide range of information from materials to devices.

How to reference

In order to correctly reference this scholarly work, feel free to copy and paste the following:

INTECH

open science | open minds